Seismic rock physics of steam injection in bituminous oil reservoirs

Evan Bianco, Sam Kaplan, and Douglas Schmitt, University of Alberta, Canada

This case study explores rock physics properties of heavy oil reservoirs subject to the steam-assisted gravity drainage (SAGD) thermal enhanced recovery process (Butler, 1998; Butler and Stephens, 1981). Previous measurements —e.g., Wang et al. (1990) and Eastwood (1993)—of the temperature-dependant properties of heavy oil-saturated sands are extended by fluid-substitution modeling and wireline data to assess the effects of pore fluid composition, and pressure and temperature changes on the seismic velocities of unconsolidated sands. Rock physics modeling is applied to a typical shallow McMurray Formation reservoir (depth of 135-160 m) within the bituminous Athabasca oil-sands deposit in western Canada to construct a rock-physics-based velocity model of the SAGD process. Although the injected steam pressure and temperature control the fluid bulk moduli within the pore space, the effective stress-dependant elastic frame moduli are the most poorly known, yet most important, factors governing the changes of seismic properties during this recovery operation. The results of the fluid substitution are used to construct a 2D synthetic seismic section to establish seismic attributes for analysis and interpretation of the physical SAGD process. The findings of this modeling promote a more complete description of 11 high-resolution, time-lapse 2D profiles over some of the earliest steam zones.

SAGD has been adopted as the recovery method of choice for producing bitumen from the Athabasca oil sands in western Canada, and it has changed relatively little since the first test installation and experiment at the Underground Test Facility in the early 1990s. The invention of this thermal EOR and horizontal drilling technology was born out of the challenges associated with producing extremely dense and viscous oil (less than 10 API) from shallow siliciclastic reservoirs. Steam carries a significant portion of its energy as latent heat, and it is much more efficient at transferring heat to the reservoir than merely circulating hot water. Engineering models of this thermal process assume that steam chamber growth is symmetric about the well pairs, but due to lithologic hetereogeneities and steam baffles, this is most certainly not the case (Figure 1).

Before seismic profiling can be optimized for tracking the movement of steam in the reservoir, it is important to understand the behavior of oil sands when subjected to elevated temperatures, pore pressure, and fluid saturation conditions resulting from SAGD.

Figure 2 shows a scanning electron micrograph (SEM) image of typical McMurray oil sand. Oil sand, by definition, lacks or has very little cementation. As such, its moduli (bulk and shear) are largely dependant upon grain-to-grain contacts. These contacts are held in place by confining pressure, and any reduction in effective pressure will result in a reduction in effective moduli. The micrographs display a subtle interlocked texture characterized by relatively high incidences of long and interpenetrative grain contacts. This suggests that

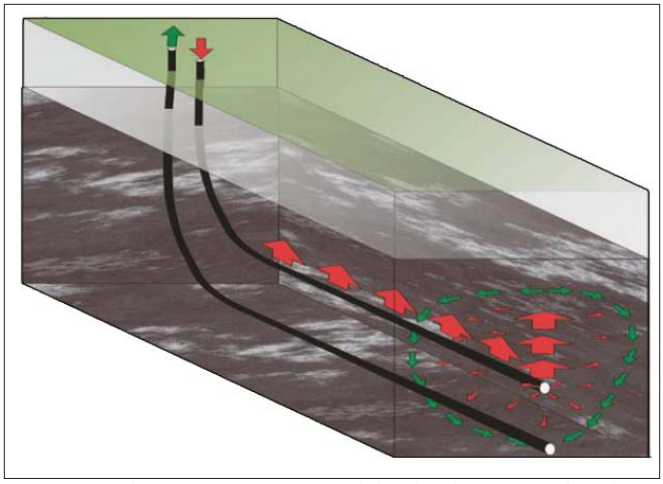

Figure 1. *Schematic representation of the plumbing system for oil drainage into horizontal well injector/producer pairs in a typical SAGD process. Steam is pumped into the top well (red arrows) and heated oil drains along the edges of a steam chamber under gravity toward a producing well along the length of the wellbore (green arrows).*

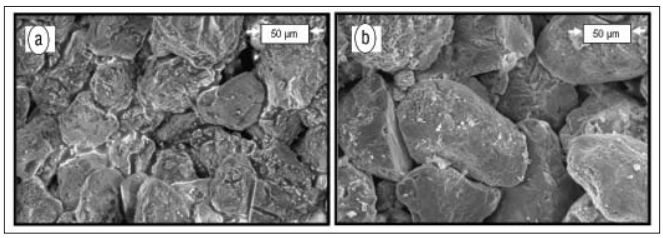

Figure 2. *SEM image of (a) uncleaned oil-sand material and (b) oil-sand material with organic components removed (cleaned). The reflective and resinous material in cracks and pores of (a) is bitumen, and trace amounts of clay can be seen in both (a) and (b).*

the shallow oil sands were once much deeper than they are today, although lithification did not occur. Furthermore, the bitumen has undergone biodegradation and is highly viscous; it may actually support the sand grains in much of this material and act as partial cement when strained at seismic frequencies.

Dipole sonic logs and density logs can provide local measurements of effective elastic properties. Effective rock properties—namely, effective P-velocity (V_P), effective S-velocity (V_S), and effective density (ρ)—are extracted from wireline data in order to establish reasonable elastic parameters (κ_{eff}, μ_{eff}, ρ) for input to Gassmann's equation for fluid substitution (Figure 3). Upon injecting steam into the reservoir, a depleted oil zone expands gradually and replaces the initial bitumen saturation with a combination of water, steam, and residual oil at elevated temperatures and pressures. Also, oil production rates are increased if the steam is injected at high pressures because the unconsolidated oil sands are deformed (although currently little is understood about what actually takes place within a steam zone). Permeability has been reported to increase as a result of geomechanical changes (e.g.,

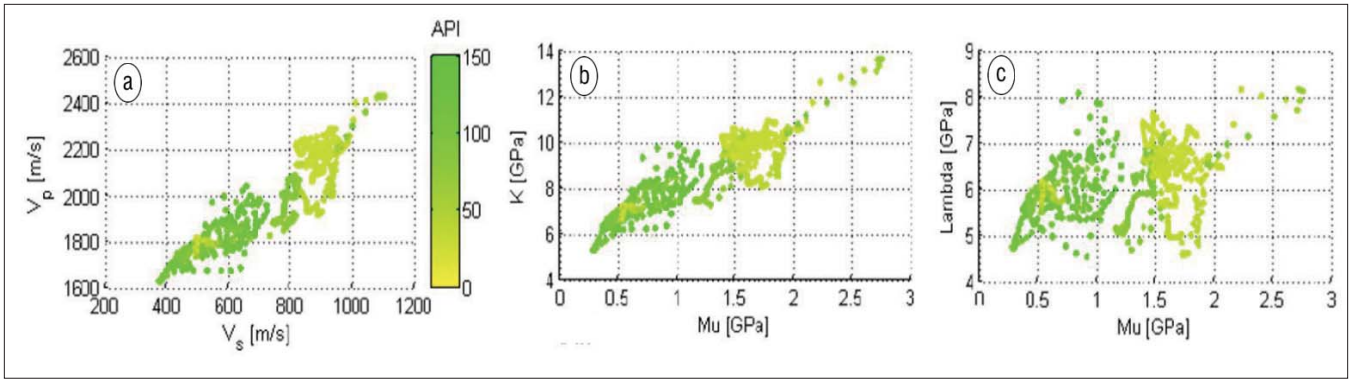

Figure 3. *Plots of (a) V_p versus V_s, (b) bulk modulus (κ) versus shear modulus (μ), and (c) incompressibility (λ) versus shear modulus (μ) computed from dipole sonic-log measurements through the McMurray Formation and the overlying mudstones of the Clearwater Formation. The color scale for each panel is tied to the gamma-ray reading (API) for each depth.*

Li and Chalaturnyk, 2006; Wong, 2003), and the portion of the reservoir that is touched by steam is completely physically altered from its original state.

In that sense, unconsolidated reservoirs cannot be treated with a simple fluid substitution calculation, and the pressure-dependant effects of the frame bulk modulus must be taken into account.

The fluid is also complicated. Ternary diagrams aid in studying the effective P-velocity response of this three-component fluid ensemble (oil, water, and steam) for a variety of temperature and pore-pressure scenarios (Figure 4). The result is a more accurate description of the in-situ elastic parameters within an idealized steam chamber, because the frame likely has been completely altered by increased pore pressure and temperature. Ternary diagrams also present a visual representation of the stability of a given effective property of interest. In this reservoir, we assume that a considerable amount of oil remains irreducibly trapped within the steam zone; the initial oil saturation of 88% falls to 62%, corresponding to a modest recovery factor of 30% within the depleted zone. If we assume that recovery is say 60%, then the resultant change in effective P-velocity of this new material is only a few percent higher. Compared to an initial velocity of 2150 m/s and a final velocity of 1506 m/s (a 30% decrease), the error associated with such a saturation range is negligible. The ternary diagram can be used to evaluate a property of interest for all possible saturation combinations of a three-component mixture.

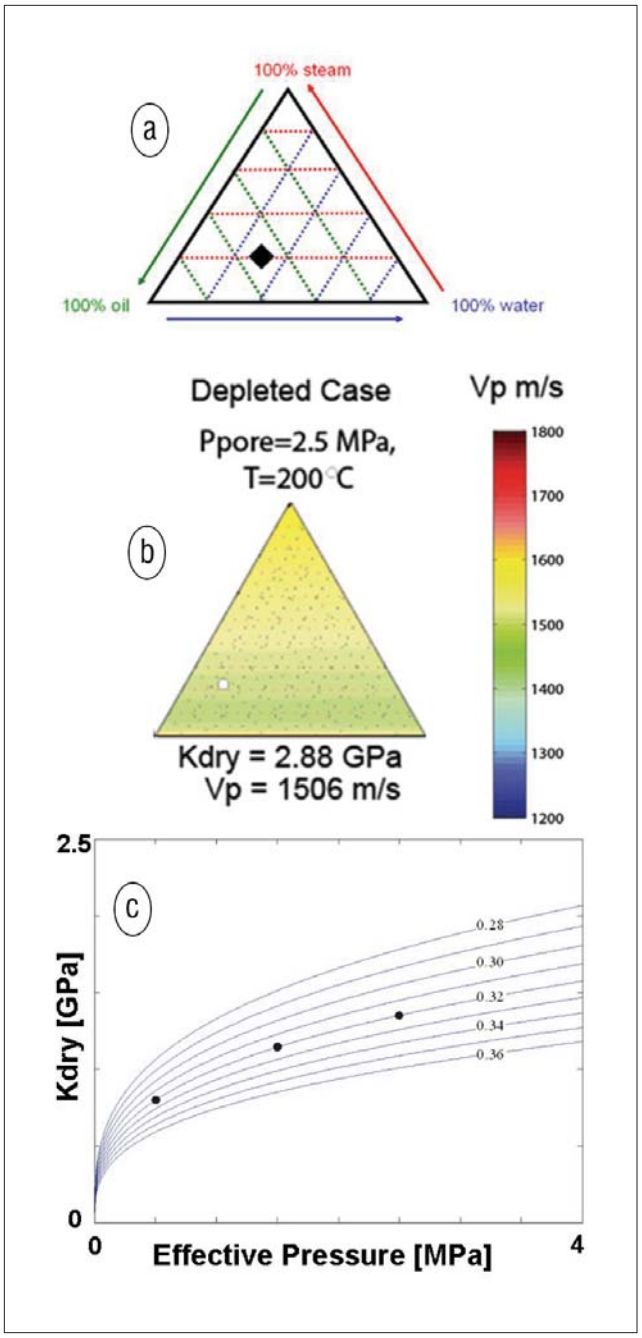

Figure 4. *Ternary diagrams can be used to plot mixture properties of three-component mixtures. The black diamond in (a) indicates a pore fluid containing 20% steam, 30% water, and 50% oil. The effective P-wave velocity has been calculated for all permutations of oil + water + steam saturation scenarios. Typical reservoir temperatures and pressures were used to estimate the change in P-wave velocity of oil sands from 2150 m/s before steam injection to 1506 m/s after steam injection (b). The pressure-dependant decrease in frame bulk modulus (K_{dry}) is computed using a modified Hertz-Mindlin formulation extrapolated from unconsolidated spherical grains (c). Curves in (c) represent typical porosities for unconsolidated materials.*

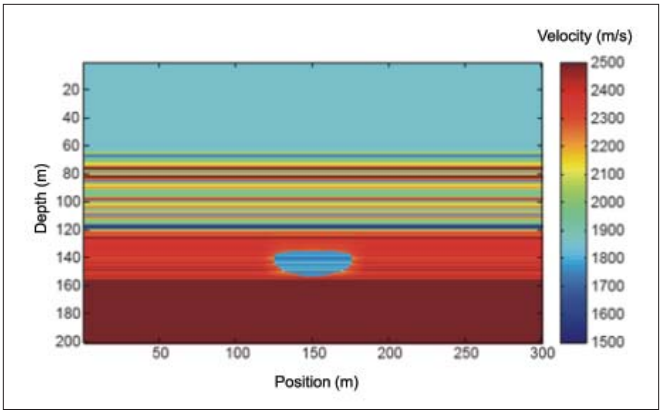

Figure 5. *High-resolution velocity model used as input for finite-difference forward modeling. The background horizontal layers are derived from closely spaced wells at the Underground Test Facility where observation wells are 40 m apart. This extremely high-density wireline sampling produces an intricate and high-resolution cross-section through a steam zone.*

Integrating rock physics and reservoir parameters for improved synthetic modeling

A background or baseline acoustic velocity model was created from a composite of logs from the general area. This "high-resolution" velocity model (Figure 5) was impregnated with the idealized velocity anomaly shown in the middle panel of Figure 6.

To explain the propagation of seismic energy through an oil-depleted steam chamber surrounded by cold, untouched, virgin reservoir, a finite-difference algorithm was employed to calculate the wavefield generated through the acoustic velocity model. Shots were collected every 2 m along the profile, and receivers were placed every 2 m on either side of the shot. The poststack image was created using conventional NMO correction and stacking with a resulting CMP spacing of 1 m (Figure 6).

The top of the steam zone is marked by a trough event, as expected, due to a strong negative reflection coefficient at the top. The base of the anomaly is marked by a strong peak event produced by an increased reflection coefficient at the bottom of the reservoir. The steam zone yields a large increase in amplitude and a significant time delay that may serve as a proxy for steam-chamber thickness. Furthermore, this example also shows that scattering plays a significant role in the seismic response with diffraction hyperbolae, complicated reverberations, and multiple reflections from within the steam zone apparent. The perturbation in the wavefield is localized about the steam zone, and internal multiples persist beneath its thickest part (~108 to ~118 m along the profile in Figure 6) for a number of cycles beneath the reservoir. Furthermore, both the top and base of the steam zone produce independent sets of remnant diffractions that remain after NMO correction and stacking have been applied. The two sets of diffractions actually have different curve shapes; the top set is faster (shallow hyperbolae), and the bottom set is slower (steeper hyperbolae). It is possible that the bottom set of diffractions are time-retarded propagation within the low-velocity steam zone, whereas the top set is not retarded and is merely scattering from the outside surface of the steam zone. These observations promote the need for 2D migration. Fomel et al. (2007) have demonstrated the ability to perform poststack migration on data using diffraction information alone, and there may be some promise to using their method, or other standard migration procedures, to actually extract quantitative time-lapse information from such features.

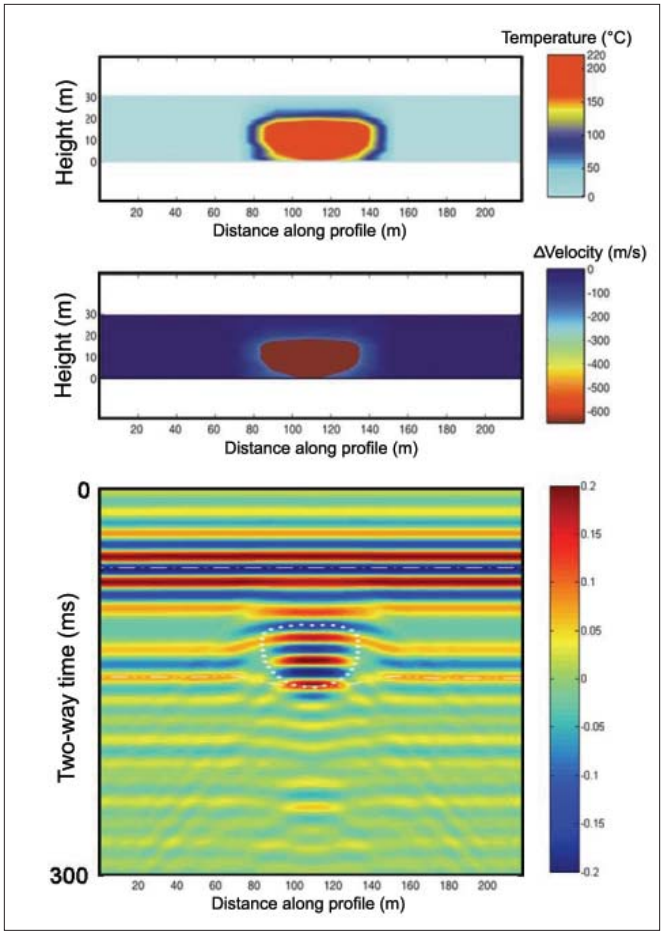

Figure 6. *(top) Temperature cross-section. (middle) Computed change in P-wave velocity from a developed steam chamber. This velocity anomaly has been inserted into a background cross-sectional velocity model for input to the finite-difference algorithm used for generating synthetic seismic data (bottom). These are poststack seismic data that have undergone conventional processing—velocity analysis, NMO correction, and stacking.*

The absence of diffractions and internal multiple events leads to a simpler and ideal image of the steam chamber. For comparison, an ideal image of the reservoir and steam zone is shown in Figure 7 where the noisy events of 2D wave propagation are not incorporated. Here, under ideal conditions, the exact shape of the steam zone can be traced out, and the geometry and volume of depleted reservoir can be accurately determined. The same is not true for the seismic section generated by finite difference. There is of course more detail, and the physics is 2D (instead of the less complete 1D convolutional model), but the final image is plagued with higher ambiguity. Here, the brightest amplitudes do not extend across the whole width of the steam zone. Direct mapping of the traveltime delay, or amplitude anomaly in this

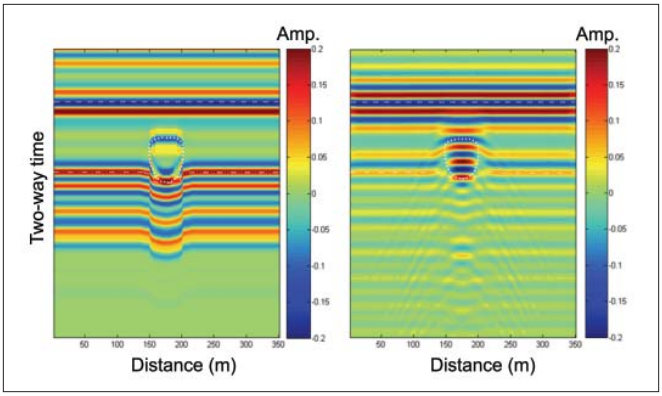

Figure 7. *Comparison between an "ideal" seismic profile (left) using simple 1D convolution, and a more realistic seismic profile over a steam zone (right) acquired using a finite-difference algorithm. The image on the right resulted from data that were densely sampled, conventionally processed, and stacked.*

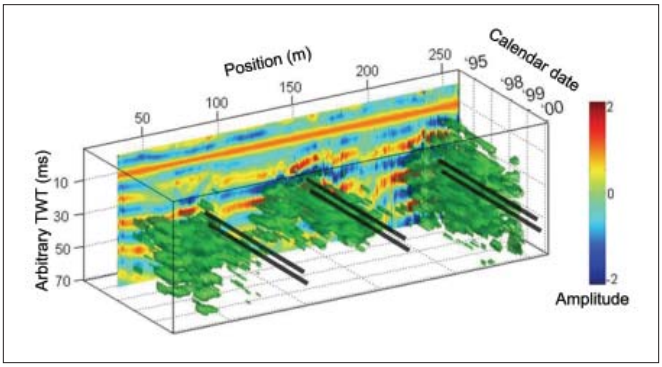

Figure 8. *3D representation of repeated 2D seismic (time-lapse) data collected over three steaming horizontal well pairs at UTF. Position and two-way traveltime are plotted on two axes and the data volume is given a "depth" perspective by stacking the repeated sections (in ascending calendar date) along the third axis. The "brightest" amplitudes (both positive and negative) have been rendered as semitransparent "iso-surfaces." These iso-surfaces are thought to be indicators of the lateral extent of the steam chambers. The reverberations are proportional to the magnitude of steam in the reservoir and coincide with the modeled reverberations in Figure 4. The approximate locations of the well pairs are indicated by the black lines; however, their size and vertical separation are not to scale.*

case, would lead the interpreter to conclude that the steam zone actually is smaller than it really is. The edge effects and resolution limits of small-scale velocity anomalies such as the one presented here must be modeled on a case-by-case basis, and simple Fresnel-zone arguments will not be sufficient in determining the maximum horizontal resolution (Schmitt, 1999). Recently, Zhang et al. (2007) presented an extensive study that shows how important adequate resolution is to characterizing such reservoirs.

Comparison with real seismic data and 2D time-lapse imaging

A series of 11 high-resolution 2D lines were collected by the University of Alberta over a five-year period at an SAGD site in northern Alberta. Due to the fact that the steam zones were relatively shallow, an exceptionally small (1 m) CMP spacing with offsets ranging from 48 to 142 m (48 channels were available and spaced 2 m apart) was used. Care was taken in repositioning the sources and receivers during these tests, and the final sections exhibit good repeatability. Figure 8 shows a volume visualization of these time-lapse data, where the "brightest" amplitudes have been highlighted as green "iso-surfaces." This image shows two interesting results that are consistent with the numerical seismic experiment: (1) the amplitude increase caused by the steam is very large and detectable, and (2) the steam anomalies are similar to the reverberation and scattering symptoms as modeled. However, the steam anomalies are not symmetric about the well pairs, (in particular the leftmost steam chamber is entirely asymmetric). Furthermore, there appears to be a sharp lateral drop-off in the amplitudes between the steam zone, and this could be attributed to the interference of diffraction energy off the top of the steam zones.

Conclusions

The oil sands of western Canada are truly unique materials and an immense resource that is only in the early stages of exploitation. In order to advance understanding of rock physics in these settings, theoretical rock physics relationships such

as Biot-Gassmann theory must be modified to account for the unconsolidated form and high viscosity of the oils. Additionally, much remains unknown about the viscoelastic behavior of oil sands and the effect that it has on seismic wave propagation. Ideally, our synthetic full-field, finite-difference experiment should be adapted to treat shear-wave and attenuation information. Such modeling would provide a more realistic depiction of wave propagation; however, there are still too many uncertainties about attenuation and viscosity characteristics at seismic frequencies to promote full viscoelastic modeling at the same scale of spatial resolution.

The results from this analysis suggest that the feasibility of seismic monitoring does not only depend on the thermal- and mechanical-related changes associated with fluid substitution, but also on the scale of the steam anomaly itself. Thorough rock physics modeling can aid in the long-term survey design for monitoring reservoir depletion. Parameters such as spatial sampling, optimal fold, repeat time intervals, and source type (to name only a few) can all be evaluated prior to first steam. Future work is required to correlate these seismic measurements to the thermocouple profiles from observation wells (e.g., Birrell, 2003), after which time the full extent and utility of such highly sampled data can be ascertained.

Suggested reading. "Heat transfer ahead of a SAGD steam chamber: A study of thermocouple data from Phase B of the UTF (Dover Project)" by Birrel (*Journal of Canadian Petroleum Technology*, 2003). "Temperature-dependant propagation of P- and S- waves in Cold Lake oil sands: Comparison of theory and experiment" by Eastwood (GEOPHYSICS, 1993). "Effect of temperature on wave velocities in sands and sandstones with heavy hydrocarbons" by Wang and Nur (SPE *Reservoir Evaluation and Engineering Journal*, 1990). "Poststack velocity analysis by separation and imaging of seismic diffractions" by Fomel et al. (GEOPHYSICS, 2007). "SAGD comes of age!" by Butler (*Journal of Canadian Petroleum Technology*, 1998). "The gravity drainage of steam-heated heavy oil to parallel horizontal wells" by Butler and Stephens (*Journal of Canadian Petroleum Technology*, 1981). "Permeability variations associated with shearing and isotropic unloading during the SAGD process" by Li and Chalatunyk (*Journal of Canadian Petroleum Technology*, 2006). "Seismic attributes for monitoring of a shallow heated heavy oil reservoir: A case study" by Schmitt (GEOPHYSICS, 1999). "A model for strain-induced permeability anisotropy in deformable granular media" by Wong (*Canadian Geotechnical Journal*, 2003). "Understanding reservoir architectures and steam-chamber growth at Christina Lake, Alberta, by using 4D seismic and crosswell seismic imaging" by Zhang et al. (SPE *Reservoir Evaluation and Engineering Journal*, 2007). TLE

Acknowledgements: Research funded via NSERC and earlier contracts from AOSTRA and COURSE.

Corresponding author: evan.m.bianco@gmail.com